

Searching for $Z_{\mu\tau}$ and h_2 in the $U(1)_{L_\mu-L_\tau}$ model at future colliders

Speaker: Jin-Xin Hou

Co-Authors: Chong-Xing Yue, Zhen-Hua Zhao and Yu-Chen Guo

Liaoning Normal University

Nanjing Normal University, Apr. 21, 2019

This report is based on our works:

"Searching for the light gauge boson $Z_{\mu\tau}$ via $t\bar{t}h_1$ production at LHC" [**Int.J.Mod.Phys.A33(2018)no.21, 1850124**].

"Searching for the light gauge boson $Z_{\mu\tau}$ via Higgstrahlung process in the $U(1)_{L_\mu-L_\tau}$ model at e^+e^- colliders"
[**Nucl.Phys.B940(2019)377 – 392**].

"Searching for $Z_{\mu\tau}$ and h_2 in the $U(1)_{L_\mu-L_\tau}$ model at the future e-p colliders" [**To be published**].

- 1 A brief review of the $U(1)_{L_\mu-L_\tau}$ model
 - 1 Source and advantages of the model
 - 2 Basic structures of the model
 - 3 Parameter space of the model
- 2 Searching for $Z_{\mu\tau}$ in the $U(1)_{L_\mu-L_\tau}$ model at e^+e^- colliders
 - 1 The production of $Z_{\mu\tau}$
 - 2 Signal and background simulation
- 3 Searching for h_2 as well as $Z_{\mu\tau}$ in the $U(1)_{L_\mu-L_\tau}$ model at e-p colliders
 - 1 The decays and productions of h_2
 - 2 The productions of $Z_{\mu\tau}$
 - 3 Signal and background simulation
- 4 Conclusions

I. A brief review of the $U(1)_{L_\mu - L_\tau}$ model

1.1. Source and advantages of the model

- The $U(1)_{L_\mu - L_\tau}$ model is a minimal extension of the SM where the SM Lagrangian has been imposed an extra local $U(1)_{L_\mu - L_\tau}$ symmetry, where the L_μ and L_τ are the muon and tau lepton numbers respectively. The complete gauge group of the model is $SU(3)_C \times SU(2)_L \times U(1)_Y \times U(1)_{L_\mu - L_\tau}$. One of the advantages of the $U(1)_{L_\mu - L_\tau}$ extension is that the anomaly cancellation does not require any extra chiral fermionic degrees of freedom.
- The spontaneous breaking of the $L_\mu - L_\tau$ symmetry generates mass for the extra neutral gauge boson $Z_{\mu\tau}$. The $Z_{\mu\tau}$ with an MeV-scale mass can resolve the muon $(g - 2)$ anomaly, explain the deficit of cosmic neutrino flux and resolve the problem of relic abundance of DM in the scenario with a light weakly interacting massive particle simultaneously.

I. A brief review of the $U(1)_{L_\mu-L_\tau}$ model

1.1. Source and advantages of the model

- The spontaneous breaking of the gauged $U(1)_{L_\mu-L_\tau}$ symmetry leads to additional terms in the right-handed neutrino mass matrix, providing a natural explanation of the neutrino masses and mixing.
- The scalar area has been expanded by two additional complex scalar singlets (ϕ_H and ϕ_{DM}) with nonzero $L_\mu - L_\tau$ charge. The scalar field ϕ_{DM} does not acquire any VEV and can act as a viable DM candidate.
- The other scalar field ϕ_H acquires a vacuum expectation value (VEV) $v_{\mu\tau}$ and thereby making an additional neutral scalar boson h_2 product after spontaneous breaking of $U(1)_{L_\mu-L_\tau}$, which indicates that the h_2 has a mass of the same order with the $v_{\mu\tau}$ about 10 GeV - 1000 GeV. The h_2 plays an important role in precise measurement of Higgs boson properties, because it can be produced and decay via their mixing with the SM-like Higgs boson h_1 .

I. A brief review of the $U(1)_{L_\mu-L_\tau}$ model

1.2. Basic structures of the model

All particles included in the $U(1)_{L_\mu-L_\tau}$ model and their charge assignments under various symmetry groups are listed in following tables:

Gauge Group	Scalar Fields			Lepton Fields								
	φ_h	φ_H	φ_{DM}	L_e	L_μ	L_τ	e_R	μ_R	τ_R	N_R^e	N_R^μ	N_R^τ
$SU(2)_L$	2	1	1	2	2	2	1	1	1	1	1	1
$U(1)_Y$	1/2	0	0	-1/2	-1/2	-1/2	-1	-1	-1	0	0	0
$U(1)_{L_\mu-L_\tau}$	0	1	$n_{\mu\tau}$	0	1	-1	0	1	-1	0	1	-1

Gauge Group	Baryon Fields											
	u_L	d_L	c_L	s_L	t_L	b_L	u_R	d_R	c_R	s_R	t_R	b_R
$SU(2)_L$	2	2	2	2	2	2	1	1	1	1	1	1
$U(1)_Y$	1/6	1/6	1/6	1/6	1/6	1/6	2/3	-1/3	2/3	-1/3	2/3	-1/3
$U(1)_{L_\mu-L_\tau}$	0	0	0	0	0	0	0	0	0	0	0	0

I. A brief review of the $U(1)_{L_\mu-L_\tau}$ model

1.2. Basic structures of the model

The complete Lagrangian for this model

$$\mathcal{L} = \mathcal{L}_{SM} + \mathcal{L}_N + \mathcal{L}_{DM} + |D_\nu \varphi_H|^2 - V - \frac{1}{4} F_{\mu\tau}^{\rho\sigma} F_{\mu\tau\rho\sigma} \quad (1)$$

The scalar potential V contains all the self interactions of ϕ_H and its interactions with SM Higgs doublet. Its expression form is given by

$$V = \mu_H^2 \varphi_H^\dagger \varphi_H + \lambda_H (\varphi_H^\dagger \varphi_H)^2 + \lambda_{hH} (\varphi_h^\dagger \varphi_h) (\varphi_H^\dagger \varphi_H). \quad (2)$$

The scalar fields φ_h and φ_H can be expanded into

$$\varphi_h = \begin{pmatrix} \frac{\tilde{H}}{\sqrt{2}} \\ \frac{v+H+iA}{\sqrt{2}} \end{pmatrix}, \quad \varphi_H = \begin{pmatrix} \frac{v_{\mu\tau} + H_{\mu\tau} + ia}{\sqrt{2}} \end{pmatrix}. \quad (3)$$

The new basis states (h_1 and h_2) are some linear combinations of H and $H_{\mu\tau}$. The new basis states, now representing two the physical states and the mixing angle between H and $H_{\mu\tau}$ can be expressed

$$h_1 = H \cos \alpha + H_{\mu\tau} \sin \alpha, \quad h_2 = -H \sin \alpha + H_{\mu\tau} \cos \alpha, \quad (4)$$

$$\tan 2\alpha = \frac{\lambda_{hH} v_{\mu\tau} v}{\lambda_h v^2 - \lambda_H v_{\mu\tau}^2}. \quad (5)$$

I. A brief review of the $U(1)_{L_{\mu}-L_{\tau}}$ model

1.2. Basic structures of the model

Relevant couplings of h_1 with the SM particles and $Z_{\mu\tau}$

$$g_{Z_{\mu\tau}Z_{\mu\tau}h_1} = \frac{2M_{Z_{\mu\tau}}^2}{v_{\mu\tau}} \sin \alpha, \quad g_{q\bar{q}h_1} = -\frac{M_q}{v} \cos \alpha, \quad g_{l\bar{l}h_1} = -\frac{M_l}{v} \cos \alpha, \\ g_{ZZh_1} = \frac{2M_Z^2 \cos \alpha}{v}, \quad g_{W^+W^-h_1} = \frac{2M_W^2 \cos \alpha}{v}.$$

Relevant couplings of h_2 with the SM particles and $Z_{\mu\tau}$

$$g_{Z_{\mu\tau}Z_{\mu\tau}h_2} = \frac{2M_{Z_{\mu\tau}}^2}{v_{\mu\tau}} \cos \alpha, \quad g_{f\bar{f}h_2} = \frac{M_f}{v} \sin \alpha, \quad g_{VVh_2} = -\frac{2M_V^2}{v} \sin \alpha, \\ g_{h_1h_1h_2} = 6v\lambda_{h_1} \cos^2 \alpha \sin \alpha - 6v_{\mu\tau}\lambda_{h_2} \sin^2 \alpha \cos \alpha - 2v\lambda_{h_1h_2} \sin \alpha \\ + 6v\lambda_{h_1h_2} \sin^3 \alpha - v_{\mu\tau}\lambda_{h_1h_2} \cos \alpha + 3v_{\mu\tau}\lambda_{h_1h_2} \sin^2 \alpha \cos \alpha.$$

I. A brief review of the $U(1)_{L_\mu-L_\tau}$ model

1.3. Parameter space of the model

The favored regions of the gauge coupling $g_{\mu\tau}$ and the $Z_{\mu\tau}$ mass to explain the muon $(g-2)$ anomaly were summarized in [arXiv:1803.00842 \[hep-ph\]](#).

$$g_{\mu\tau} \simeq [2 \times 10^{-4}, 2 \times 10^{-3}], \quad M_{Z_{\mu\tau}} \simeq [5, 210] \text{ MeV}, \quad (6)$$

$$v_{\mu\tau} = \frac{M_{Z_{\mu\tau}}}{g_{\mu\tau}} \simeq [10, 1000] \text{ GeV}. \quad (7)$$

The sine of scalar mixing angle $\sin \alpha$ and the branching ratio of invisible decay of Higgs, BR_{invis} at 95% C. L., are also constrained by analysis of data from the LHC experiment [[arXiv:1307.3948 \[hep-ph\]](#) and [arXiv:1507.06158 \[hep-ph\]](#)] as

$$\sin \alpha \leq 0.3, \quad \text{BR}_{\text{invis}} \leq 0.24, \quad (8)$$

$$\chi = \frac{\alpha}{v_{\mu\tau}} \leq 2.2 \times 10^{-4} \text{ GeV}^{-1}. \quad (9)$$

II. Searching for $Z_{\mu\tau}$ in the $U(1)_{L_\mu-L_\tau}$ model at e^+e^- colliders

2.1. The production of $Z_{\mu\tau}$

The $Z_{\mu\tau}$ can not establish the couplings with quarks and the electron family, making it very difficult to be produced directly. So it is a good choice to consider the indirect production of $Z_{\mu\tau}$. Besides decaying to the SM particles, the SM-like Higgs boson h_1 has an extra decay mode to a pair of $Z_{\mu\tau}$ within this framework.

The expression of decay width of $h_1 \rightarrow Z_{\mu\tau}Z_{\mu\tau}$ is given by

$$\Gamma(h_1 \rightarrow Z_{\mu\tau}Z_{\mu\tau}) = \frac{M_{h_1}^4 - 4M_{Z_{\mu\tau}}^2 M_{h_1}^2 + 12M_{Z_{\mu\tau}}^2}{128\pi M_{h_1}^2 M_{Z_{\mu\tau}}^4} * g_{h_1 Z_{\mu\tau} Z_{\mu\tau}}^2 \sqrt{M_{h_1}^2 - 4M_{Z_{\mu\tau}}^2} \quad (10)$$

After simplification ($\frac{M_{Z_{\mu\tau}}}{M_{h_1}} \rightarrow 0$), we can get

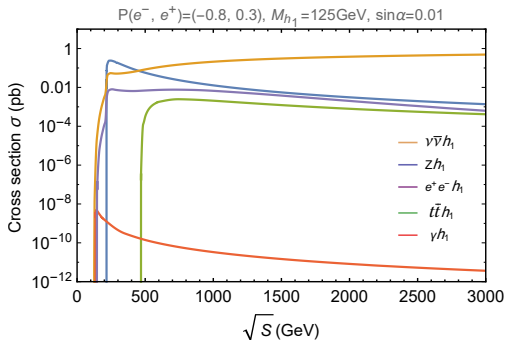
$$\Gamma(h_1 \rightarrow Z_{\mu\tau}Z_{\mu\tau}) = \frac{M_{h_1}^3 \sin^2 \alpha}{32\pi v_{\mu\tau}^2} \quad (11)$$

The Eq. (11) indicates that the $Z_{\mu\tau}$ pair production rate is actually determined by the factor $\chi^2 \simeq \sin^2 \alpha / v_{\mu\tau}^2$. For this, this section will emphasize on the research of the production of $Z_{\mu\tau}$ via the h_1 decay and all the results in this section can be expressed as functions of χ .

II. Searching for $Z_{\mu\tau}$ in the $U(1)_{L_\mu-L_\tau}$ model at e^+e^- colliders

2.1. The production of $Z_{\mu\tau}$

The cross sections of SM-like Higgs boson's different production channels which depend on the c.m. energy are calculated at the tree level by employing Madgraph5/aMC@NLO

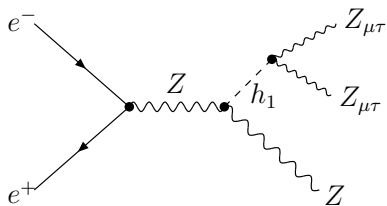


- $e^+e^- \rightarrow Zh_1$ and $e^+e^- \rightarrow \nu\bar{\nu}h_1$ have the largest cross sections which are several orders of magnitude larger than those for the other three processes.
- $Z_{\mu\tau}$ can only decay to neutrinos in this framework, so the $e^+e^- \rightarrow \nu\bar{\nu}h_1 (h_1 \rightarrow Z_{\mu\tau}Z_{\mu\tau})$ process has an invisible final state.
- The $e^+e^- \rightarrow Zh_1$ process which has the leptonic and the hadronic final states (arising from $Z \rightarrow l^+l^-$ and $Z \rightarrow jj$, respectively) is worthy of our in-depth analysis.

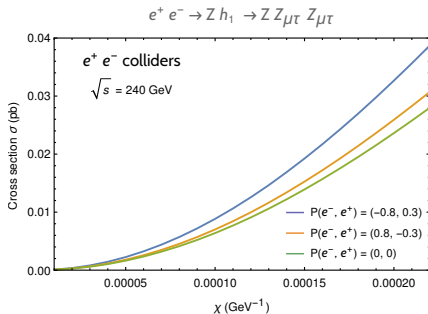
II. Searching for $Z_{\mu\tau}$ in the $U(1)_{L_\mu-L_\tau}$ model at e^+e^- colliders

2.1. The production of $Z_{\mu\tau}$

The Feynman diagram of gauge boson $Z_{\mu\tau}$ production by the h_1 decay via the $Z h_1$ associated production at the e^+e^- colliders (a). The cross sections of $Z_{\mu\tau}$ production as functions of the factor χ at the 240 GeV e^+e^- colliders. The solid curves show the cross sections of the $e^+e^- \rightarrow Z h_1 \rightarrow Z Z_{\mu\tau} Z_{\mu\tau}$ process with different polarizations $P(e^-, e^+) = (-0.8, 0.3)$ (blue), $P(e^-, e^+) = (0.8, -0.3)$ (orange) and $P(e^-, e^+) = (0, 0)$ (green) (b).



(a)



(b)

II. Searching for $Z_{\mu\tau}$ in the $U(1)_{L_\mu-L_\tau}$ model at e^+e^- colliders

2.2. Signal and background simulation

Signals and backgrounds

1 Two kinds of signals

- $e^+e^- \rightarrow Z(\rightarrow l^+l^-)h_1(\rightarrow Z_{\mu\tau}Z_{\mu\tau}) \rightarrow l^+l^- + \cancel{E}_T$, **Leptonic Signal**
- $e^+e^- \rightarrow Z(\rightarrow jj)h_1(\rightarrow Z_{\mu\tau}Z_{\mu\tau}) \rightarrow jj + \cancel{E}_T$, **Hadronic Signal**

2 Corresponding SM background processes of leptonic channel

- $e^+e^- \rightarrow Z(\rightarrow l^+l^-)Z(\rightarrow \nu\nu) \rightarrow l^+l^-\nu\bar{\nu}$
- $e^+e^- \rightarrow W^+(\rightarrow l^+\nu)W^-(\rightarrow l^-\bar{\nu}) \rightarrow l^+l^-\nu\bar{\nu}$
- $e^+e^- \rightarrow \tau^+(\rightarrow e^+\nu_e)\tau^-(\rightarrow e^-\bar{\nu}_e) \rightarrow e^+e^-\nu_e\bar{\nu}_e$
add process $e^+e^- \rightarrow \tau^+(\rightarrow \mu^+\nu_\mu)\tau^-(\rightarrow \mu^-\bar{\nu}_\mu) \rightarrow \mu^+\mu^-\nu_\mu\bar{\nu}_\mu$

3 Corresponding SM background processes of hadronic channel

- $e^+e^- \rightarrow Z(\rightarrow jj)Z(\rightarrow \nu\nu) \rightarrow jj\nu\bar{\nu}$
- $e^+e^- \rightarrow \tau^+\tau^-$

II. Searching for $Z_{\mu\tau}$ in the $U(1)_{L_\mu-L_\tau}$ model at e^+e^- colliders

2.2. Signal and background simulation

The signal and background events are generated with following basic cuts implemented in Madgraph5/aMC@NLO.

The basic selection cuts for leptonic signal

- lepton transverse momentum $p_T(l^\pm) > 10$ GeV ,
- lepton pseudorapidity in the range $|\eta(l^\pm)| < 2.5$,
- missing transverse energy $\cancel{E}_T > 10$ GeV ,
- angular separation between any two objects $\Delta R > 0.2$.

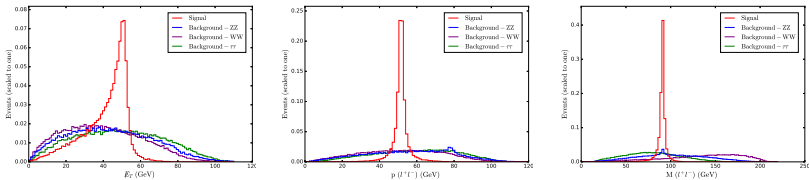
The basic selection cuts for hadronic signal

- jet transverse momentum $p_T(j) > 20$ GeV ,
- jet pseudorapidity in the range $|\eta(j)| < 5.0$,
- missing transverse energy $\cancel{E}_T > 10$ GeV ,
- angular separation between any two objects $\Delta R > 0.4$.

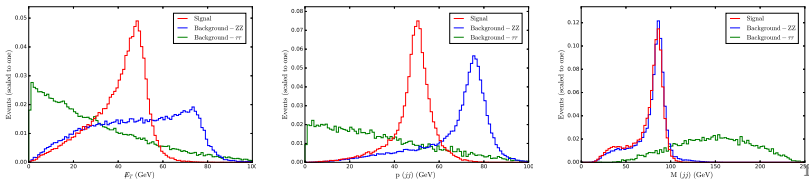
II. Searching for $Z_{\mu\tau}$ in the $U(1)_{L_{\mu}-L_{\tau}}$ model at e^+e^- colliders

2.2. Signal and background simulation

- Normalized distributions of \cancel{E}_T , $p(l^+l^-)$ and $M(l^+l^-)$ for the leptonic signal and backgrounds at the e^+e^- colliders with $\sqrt{s} = 240$ GeV and an integrated luminosity of 5 ab^{-1} .



- Normalized distributions of \cancel{E}_T , $p(l^+l^-)$ and $M(l^+l^-)$ for the hadronic signal and backgrounds at the e^+e^- colliders with $\sqrt{s} = 240$ GeV and an integrated luminosity of 5 ab^{-1} .



II. Searching for $Z_{\mu\tau}$ in the $U(1)_{L_\mu-L_\tau}$ model at e^+e^- colliders

2.2. Signal and background simulation

- Effect of individual kinematical cuts on the leptonic signal for $\chi = 9 \times 10^{-5} \text{ GeV}^{-1}$ ($M_{Z_{\mu\tau}} = 0.1 \text{ GeV}$, $\sin\alpha = 0.01$ and $g_{\mu\tau} = 9 \times 10^{-4}$) and backgrounds. The SS is computed for a luminosity of 5 ab^{-1} (300 fb^{-1}).

e^+e^- colliders, $\sqrt{s} = 240 \text{ GeV}$, $P(e^-, e^+) = (-0.8, 0.3)$

Cuts	Signal (S)	Total background (B)	$S/\sqrt{S+B}$
Initial (no cut)	2210 (132)	1.59×10^7 (9.52×10^5)	0.56 (0.14)
Basic cuts	1674.6 (100.48)	1.21×10^7 (7.29×10^5)	0.48 (0.12)
30 GeV $< \mathcal{E}'_T < 55 \text{ GeV}$	1343.5 (80.61)	4.94×10^6 (2.97×10^5)	0.60 (0.15)
45 GeV $< p(l^+l^-) < 55 \text{ GeV}$	1193.4 (71.61)	1.48×10^6 (8.89×10^4)	0.98 (0.24)
$ M(l^+l^-) - M_Z < 10 \text{ GeV}$	1186.5 (71.19)	1.47×10^5 (8.85×10^3)	3.08 (0.75)

- Effect of individual kinematical cuts on the hadronic signal for $\chi = 9 \times 10^{-5} \text{ GeV}^{-1}$ ($M_{Z_{\mu\tau}} = 0.1 \text{ GeV}$, $\sin\alpha = 0.01$ and $g_{\mu\tau} = 9 \times 10^{-4}$) and backgrounds. The SS is computed for a luminosity of 5 ab^{-1} (300 fb^{-1}).

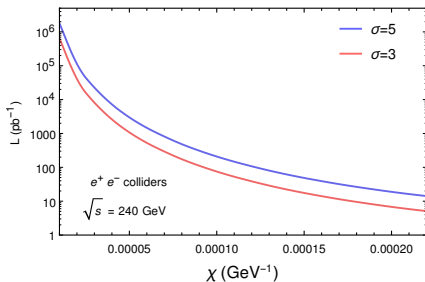
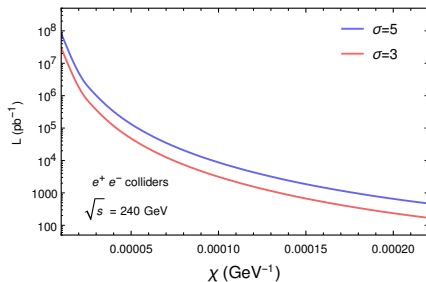
e^+e^- colliders, $\sqrt{s} = 240 \text{ GeV}$, $P(e^-, e^+) = (-0.8, 0.3)$

Cuts	Signal (S)	Total background (B)	$S/\sqrt{S+B}$
Initial (no cut)	17235 (1034)	1.49×10^7 (8.94×10^5)	4.46 (1.09)
Basic cuts	11944 (716.7)	2.94×10^6 (1.77×10^5)	6.94 (1.70)
35 GeV $< \mathcal{E}'_T < 55 \text{ GeV}$	9173.2 (550.4)	1.02×10^6 (6.09×10^4)	9.06 (2.22)
40 GeV $< p(jj) < 60 \text{ GeV}$	8460.3 (507.6)	3.91×10^5 (2.35×10^4)	13.38 (3.28)
$ M(jj) - M_Z < 10 \text{ GeV}$	5541.4 (332.5)	7.02×10^4 (4.21×10^3)	20.13 (4.93)

II. Searching for $Z_{\mu\tau}$ in the $U(1)_{L_\mu-L_\tau}$ model at e^+e^- colliders

2.2. Signal and background simulation

Integrated luminosity required for observing the $Z_{\mu\tau}$ at the 3σ (red line) and 5σ (blue line) statistical significances at different values of χ at the 240 GeV e^+e^- colliders (Left: for the leptonic channel, Right: for the hadronic channel).



The statistical significance of hadronic channel is much higher than that of leptonic channel. This is due to the facts that there is a higher number of signal events by $Br(Z \rightarrow jj) > Br(Z \rightarrow l^+l^-)$ and the $e^+e^- \rightarrow W^+W^-$ process does not contribute to the hadronic mode's backgrounds.

III. Searching for the h_2 as well as $Z_{\mu\tau}$ in the $U(1)_{L_\mu-L_\tau}$ model at e-p colliders

3.1. The decays and productions of h_2

The decay width expressions of h_2 's several major decay modes

$$\Gamma(h_2 \rightarrow Z_{\mu\tau} Z_{\mu\tau}) = \frac{g_{h_2 Z_{\mu\tau} Z_{\mu\tau}}^2 (M_{h_2}^4 - 4M_{Z_{\mu\tau}}^2 M_{h_2}^2 + 12M_{Z_{\mu\tau}}^2) \sqrt{M_{h_2}^2 - 4M_{Z_{\mu\tau}}^2}}{128\pi M_{h_2}^2 M_{Z_{\mu\tau}}^4}. \quad (12)$$

$$\Gamma(h_2 \rightarrow VV) = \frac{g_{h_2 VV}^2 (M_{h_2}^4 - 4M_V^2 M_{h_2}^2 + 12M_V^2) \sqrt{M_{h_2}^2 - 4M_V^2}}{64\pi S_V M_{h_2}^2 M_V^4}, \quad (13)$$

where the S_V represents the statistical factor. Its value equal to 1 for W^\pm boson and 2 for Z boson.

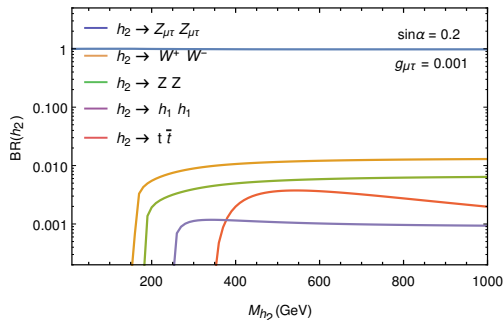
$$\Gamma(h_2 \rightarrow h_1 h_1) = \frac{g_{h_1 h_1 h_2}^2 \sqrt{M_{h_2}^2 - 4M_{h_1}^2}}{32\pi M_{h_2}^2}. \quad (14)$$

$$\Gamma(h_2 \rightarrow f\bar{f}) = \frac{n_c g_{h_2 f\bar{f}} (M_{h_2}^2 - 4M_f^2)^{\frac{3}{2}}}{8\pi M_{h_2}^2}. \quad (15)$$

III. Searching for the h_2 as well as $Z_{\mu\tau}$ in the $U(1)_{L_\mu-L_\tau}$ model at e-p colliders

3.1. The decay and production of h_2

The dominant branching ratios of the scalar boson h_2 decay as a function of M_{h_2} for a fixed value of $\sin\alpha = 0.2$, $g_{\mu\tau} = 1 \times 10^{-3}$.



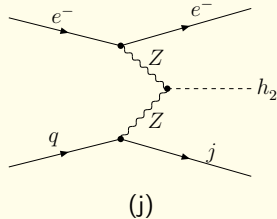
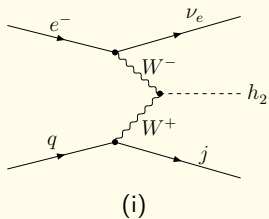
The branching ratio value of the decay channel $h_2 \rightarrow Z_{\mu\tau} Z_{\mu\tau}$ is about 98% and the rest decay channels account for 2%. So the decay channel $h_2 \rightarrow Z_{\mu\tau} Z_{\mu\tau}$ is the most dominant decay mode of the the scalar boson h_2 and we will choose it to study the feasibility of detecting h_2 .

III. Searching for the h_2 as well as $Z_{\mu\tau}$ in the $U(1)_{L_\mu-L_\tau}$ model at e-p colliders

3.1. The decay and production of h_2

Like the Higgs boson in the SM, the additional scalar boson h_2 in the $U(1)_{L_\mu-L_\tau}$ model is produced via two major channels: the charged current (CC) production channel via W^+W^- fusion and the neutral current (NC) production channel via ZZ fusion at e-p colliders.

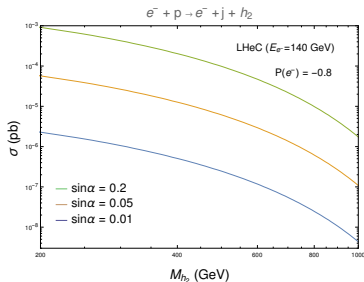
The Feynman diagrams of the scalar boson h_2 products at the e-p colliders (Left: CC production channel, Right: NC production channel).



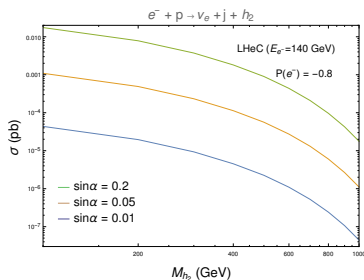
III. Searching for the h_2 as well as $Z_{\mu\tau}$ in the $U(1)_{L_\mu-L_\tau}$ model at e-p colliders

3.1. The decays and productions of h_2

The cross sections of the h_2 production as a function of M_{h_2} from the process $e^- p \rightarrow e^- j h_2$ and the $e^- p \rightarrow e^- \nu_e h_2$ for $\sin \alpha = 0.2$ (green), $\sin \alpha = 0.05$ (orange) and $\sin \alpha = 0.01$ (blue) with $P(e^-) = -0.8$ at LHeC.



(k)



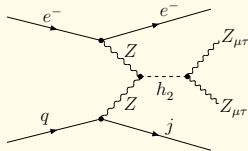
(l)

The cross section of $e^- p \rightarrow \nu_e j h_2$ process is one order of magnitude larger than the cross section of $e^- p \rightarrow e^- j h_2$ process.

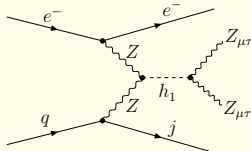
III. Searching for the h_2 as well as $Z_{\mu\tau}$ in the $U(1)_{L_\mu-L_\tau}$ model at e-p colliders

3.2. The productions of $Z_{\mu\tau}$

$Z_{\mu\tau}$ can only decay to neutrinos in this framework. So the $e^-p \rightarrow \nu_e j h_2 (h_2 \rightarrow Z_{\mu\tau} Z_{\mu\tau})$ and $e^-p \rightarrow \nu_e j h_1 (h_1 \rightarrow Z_{\mu\tau} Z_{\mu\tau})$ processes end up generating a lot of jets and missing energy, which are difficult to be distinguished from the deeply inelastic scattering (DIS) background. Moreover, the lack of kinematic handles in the final state makes it extremely difficult to filter signal from many backgrounds. Therefore in this work we will focus on NC production channels $e^-p \rightarrow e^- j h_1 (\rightarrow Z_{\mu\tau} Z_{\mu\tau}) \rightarrow e^- j + \cancel{E}_T$ and $e^-p \rightarrow e^- j h_2 (\rightarrow Z_{\mu\tau} Z_{\mu\tau}) \rightarrow e^- j + \cancel{E}_T$ to study the feasibility of detecting the h_2 and $Z_{\mu\tau}$.



(m)



(n)

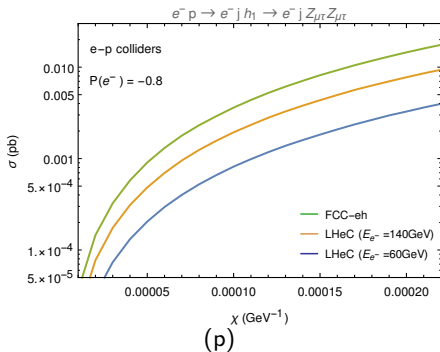
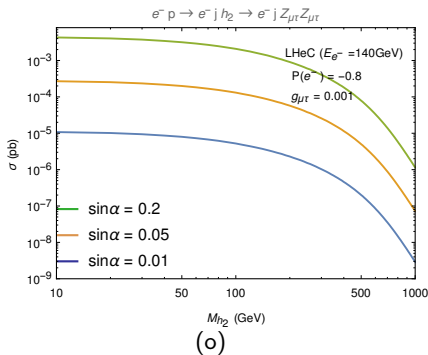
The Feynman diagrams of the gauge boson $Z_{\mu\tau}$ production by the decay of h_1 and h_2 via the NC production channel at e-p colliders.

III. Searching for the h_2 as well as $Z_{\mu\tau}$ in an $U(1)_{L_\mu-L_\tau}$ model at e-p colliders

3.2. The production of $Z_{\mu\tau}$

Left (o): The cross sections of $Z_{\mu\tau}$ production process $e^- p \rightarrow e^- j h_2 \rightarrow e^- j Z_{\mu\tau} Z_{\mu\tau}$ as functions of M_{h_2} with different $\sin\alpha$ for $g_{\mu\tau} = 1 \times 10^{-3}$ and $M_{Z_{\mu\tau}} = 0.1$ GeV at the LHeC with $E_{e^-} = 140$ GeV.

Right (p): The cross sections of $Z_{\mu\tau}$ production process $e^- p \rightarrow e^- j h_1 \rightarrow e^- j Z_{\mu\tau} Z_{\mu\tau}$ as a function of χ at the e-p colliders.



III. Searching for the h_2 as well as $Z_{\mu\tau}$ in the $U(1)_{L_\mu-L_\tau}$ model at e-p colliders

3.3. Signal and background simulation

Signals and backgrounds

① Two kinds of signals

- $e^- + p \rightarrow e^- + j + h_2(\rightarrow Z_{\mu\tau}Z_{\mu\tau}) \rightarrow e^- + j + \cancel{E}_T$, **Signal-1**
- $e^- + p \rightarrow e^- + j + h_1(\rightarrow Z_{\mu\tau}Z_{\mu\tau}) \rightarrow e^- + j + \cancel{E}_T$. **Signal-2**

② Corresponding SM background processes of leptonic channel

- $e^- + p \rightarrow W^-(\rightarrow e^-\bar{\nu}_e) + j + \nu_e \rightarrow e^- + j + \cancel{E}_T$
add process $e^- + p \rightarrow Z(\rightarrow \nu_e\bar{\nu}_e) + j + e^- \rightarrow e^- + j + \cancel{E}_T$, $(e^- j \nu_e \bar{\nu}_e)$
- $e^- + p \rightarrow Z(\rightarrow \nu_{\mu,\tau}\bar{\nu}_{\mu,\tau}) + j + e^- \rightarrow e^- + j + \cancel{E}_T$, $(e^- j \nu_{\mu,\tau}\bar{\nu}_{\mu,\tau})$
- $e^- + p \rightarrow e^- + j + \tau^+ + \nu_\tau$, $(e^- j \tau^+ \nu_\tau)$
- $e^- + p \rightarrow e^- + j + \tau^- + \bar{\nu}_\tau$. $(e^- j \tau^- \bar{\nu}_\tau)$

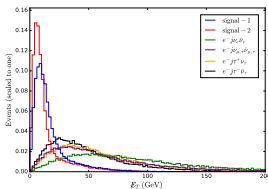
The basic selection cuts

- $p_T(l^\pm) > 5 \text{ GeV}$, $p_T(j) > 20 \text{ GeV}$, $|\eta(l^\pm)| < 5$, $|\eta(j)| < 5$, $\Delta R(jl^\pm) > 0.4$.

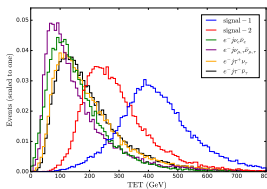
III. Searching for the h_2 as well as $Z_{\mu\tau}$ in the $U(1)_{L_\mu-L_\tau}$ model at e-p colliders

3.3. Signal and background simulation

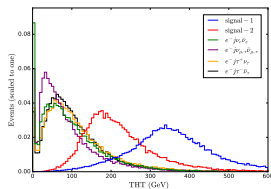
- Normalized distributions of \cancel{E}_T (q), TET (r), THT (s), $E_T(jj)$ (t) and $E_T(e^-j)$ (u) for the signal and backgrounds at the LHeC with $E_{e^-} = 140$ GeV and an integrated luminosity of 1 ab^{-1} .



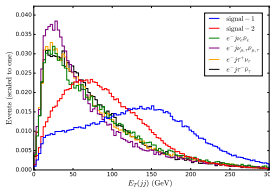
(q)



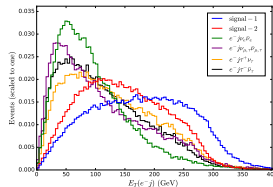
(r)



(s)



(t)



(u)

III. Searching for the h_2 as well as $Z_{\mu\tau}$ in the $U(1)_{L_\mu-L_\tau}$ model at e-p colliders

3.3. Signal and background simulation

- Effect of individual kinematical cuts on the signal-1 for $M_{h_2} = 300$ GeV, $M_{Z_{\mu\tau}} = 0.1$ GeV, $\sin\alpha = 0.2$ and $g_{\mu\tau} = 1 \times 10^{-3}$ and backgrounds at the LHeC with $E_{e^-} = 140$ (60) GeV. The statistical significance is computed for a luminosity of 1 ab^{-1} .

LHeC, $E_{e^-} = 140$ (60) GeV, $E_p = 7$ TeV, $P(e^-) = -0.8$			
cuts	signal (S)	total background (B)	$S/\sqrt{S+B}$
initial (no cut)	417.0 (104.0)	1.01×10^6 (5.09×10^5)	0.41 (0.15)
basic cuts	392.1 (97.6)	8.53×10^5 (4.11×10^5)	0.42 (0.16)
$\cancel{E}_T < 20$ ($\cancel{E}'_T < 20$) GeV	238.6 (70.7)	5.17×10^4 (4.89×10^4)	1.05 (0.32)
TET > 300 (TET > 260) GeV	235.9 (64.6)	1.65×10^4 (4.63×10^3)	1.83 (0.94)
THT > 200 (THT > 200) GeV	235.7 (63.8)	9.91×10^3 (1.42×10^3)	2.30 (1.65)
$E_T(jj) > 100$ ($E_T(jj) > 90$) GeV	232.7 (60.4)	7.83×10^3 (1.08×10^3)	2.59 (1.79)
$E_T(e^-j) > 150$ ($E_T(e^-j) > 120$) GeV	232.3 (59.5)	7.44×10^3 (9.93×10^2)	2.65 (1.84)

- Effect of individual kinematical cuts on the signal-2 for $M_{h_1} = 125$ GeV, $M_{Z_{\mu\tau}} = 0.1$ GeV, $\sin\alpha = 0.01$ and $g_{\mu\tau} = 1 \times 10^{-3}$ ($\chi = 9 \times 10^{-5} \text{ GeV}^{-1}$) and backgrounds at the LHeC with $E_{e^-} = 140$ (60) GeV. The statistical significance is computed for a luminosity of 1 ab^{-1} .

LHeC, $E_{e^-} = 140$ (60) GeV, $E_p = 7$ TeV, $P(e^-) = -0.8$			
cuts	signal (S)	total background (B)	$S/\sqrt{S+B}$
initial (no cut)	1288.0 (544.0)	1.01×10^6 (5.09×10^5)	1.28 (0.76)
basic cuts	1205.9 (508.1)	8.53×10^5 (4.11×10^5)	1.30 (0.79)
$\cancel{E}_T < 20$ ($\cancel{E}'_T < 18$) GeV	980.9 (386.0)	8.79×10^4 (4.05×10^4)	3.29 (1.91)
TET > 200 (TET > 160) GeV	827.7 (361.9)	2.26×10^4 (1.27×10^4)	5.41 (3.16)
THT > 140 (THT > 120) GeV	808.1 (354.3)	1.20×10^4 (6.09×10^3)	7.14 (4.41)
$E_T(jj) > 60$ ($E_T(jj) > 60$) GeV	803.5 (374.8)	9.65×10^3 (4.46×10^3)	7.86 (5.02)
$E_T(e^-j) > 100$ ($E_T(e^-j) > 80$) GeV	796.1 (343.7)	8.96×10^3 (4.19×10^3)	8.06 (5.10)

III. Searching for the h_2 as well as $Z_{\mu\tau}$ in the $U(1)_{L_{\mu}-L_{\tau}}$ model at e-p colliders

3.3. Signal and background simulation

- Effect of individual kinematical cuts on the signal-1 for $M_{h_2} = 300$ GeV, $M_{Z_{\mu\tau}} = 0.1$ GeV, $\sin\alpha = 0.2$ and $g_{\mu\tau} = 1 \times 10^{-3}$ and backgrounds at the FCC-eh. The statistical significance is computed for a luminosity of 1 ab^{-1} .

FCC-eh, cuts	$E_{e^-} = 60$ GeV, signal (S)	$E_p = 50$ TeV, total background (B)	$P(e^-) = -0.8$ $S/\sqrt{S+B}$
initial (no cut)	925.0	1.81×10^6	0.69
basic cuts	863.3	1.30×10^6	0.76
$\cancel{E}_T < 20$ GeV	303.2	1.29×10^5	0.84
TET > 280 GeV	279.1	1.35×10^4	2.38
THT > 200 GeV	277.7	7.34×10^3	3.18
$E_T(jj) > 100$ GeV	263.7	5.84×10^3	3.38
$E_T(e^-j) > 120$ GeV	261.9	5.61×10^3	3.42

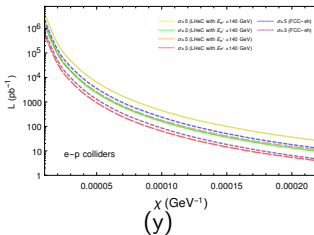
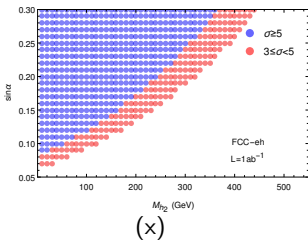
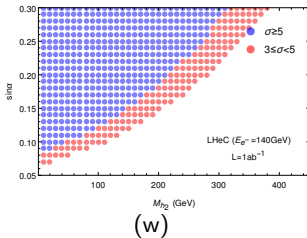
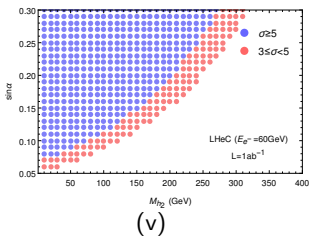
- Effect of individual kinematical cuts on the signal-2 for $M_{h_1} = 125$ GeV, $M_{Z_{\mu\tau}} = 0.1$ GeV, $\sin\alpha = 0.01$ and $g_{\mu\tau} = 1 \times 10^{-3}$ ($\chi = 9 \times 10^{-5} \text{ GeV}^{-1}$) and backgrounds at the FCC-eh. The statistical significance is computed for a luminosity of 1 ab^{-1} .

FCC-eh, cuts	$E_{e^-} = 60$ GeV, signal (S)	$E_p = 50$ TeV, total background (B)	$P(e^-) = -0.8$ $S/\sqrt{S+B}$
initial (no cut)	2412.0	1.82×10^6	1.79
basic cuts	2246.7	1.30×10^6	1.96
$\cancel{E}_T < 20$ GeV	1086.9	1.29×10^5	3.01
TET > 180 GeV	981.0	3.76×10^4	5.00
THT > 120 GeV	972.0	2.46×10^4	6.08
$E_T(jj) > 60$ GeV	959.3	1.92×10^4	6.76
$E_T(e^-j) > 80$ GeV	952.9	1.79×10^4	6.94

III. Searching for the h_2 as well as $Z_{\mu\tau}$ in the $U(1)_{L_\mu-L_\tau}$ model at e-p colliders

3.3. Signal and background simulation

- 3σ and 5σ detection potential regions for the signal-1 at the LHeC with $E_{e^-} = 60$ GeV (v), LHeC with $E_{e^-} = 140$ GeV (w) and FCC-eh (x) with an integrated luminosity of 1 ab^{-1} , respectively. Integrated luminosity required for observing the signal-2 at the 3σ and 5σ statistical significances at different values of χ at e-p colliders (y).



III. Searching for the h_2 as well as $Z_{\mu\tau}$ in the $U(1)_{L_\mu-L_\tau}$ model at e-p colliders

3.3. Signal and background simulation

For $\sin \alpha \leq 0.3$, the h_2 mass region of above 3σ statistical significance

- $10 \text{ GeV} \leq M_{h_2} \leq 320 \text{ GeV}$ (LHeC with $E_{e^-} = 60 \text{ GeV}$),
- $10 \text{ GeV} \leq M_{h_2} \leq 400 \text{ GeV}$ (LHeC with $E_{e^-} = 140 \text{ GeV}$),
- $10 \text{ GeV} \leq M_{h_2} \leq 480 \text{ GeV}$ (FCC-eh).

For $\sin \alpha \leq 0.3$, the h_2 mass region of above 5σ statistical significance

- $10 \text{ GeV} \leq M_{h_2} \leq 270 \text{ GeV}$ (LHeC with $E_{e^-} = 60 \text{ GeV}$),
- $10 \text{ GeV} \leq M_{h_2} \leq 310 \text{ GeV}$ (LHeC with $E_{e^-} = 140 \text{ GeV}$),
- $10 \text{ GeV} \leq M_{h_2} \leq 360 \text{ GeV}$ (FCC-eh).

we can obtain larger significance for larger χ values within its limit and can easily obtain 5σ statistical significance when we take $\chi \geq 5 \times 10^{-5}$ within the e-p colliders designed luminosity region. In addition, by contrast, the LHeC with $E_{e^-} = 140 \text{ GeV}$ has the best sensitivity to the signal-2.

VI. Conclusions

- We find that both the leptonic and hadronic signals considerably contribute to detecting the signature of $Z_{\mu\tau}$ with a sufficient integrated luminosity and proper values of χ at the 240 GeV e^+e^- colliders, but with a quite higher potentiality for the hadronic mode.
- Performing the scan over the parameter space, we find that the possible signature of h_2 and $Z_{\mu\tau}$ from signal-1 is limited in the lower M_{h_2} range and could be detected at the e-p colliders with an integrated luminosity of 1 ab^{-1} . On the other side, the FCC-eh could offer better detection capabilities than LHeC under the same integrated luminosity.
- Studying the signal-2, we find that the signature of $Z_{\mu\tau}$ might be easily detected at e-p colliders and the LHeC with $E_{e^-} = 140 \text{ GeV}$ has the best sensitivity to the signal-2.



$$\mu_h = \frac{\sigma_h \times \text{BR}_h}{(\sigma_h \times \text{BR}_h)_{\text{SM}}} = \kappa^2, \quad \kappa'^2 = 1 - \mu_h,$$

$$\mu_H = \frac{\sigma_H \times \text{BR}_H}{(\sigma_H \times \text{BR}_H)_{\text{SM}}} = \kappa'^2 (1 - \text{BR}_{H,\text{new}}).$$

From arXiv: 1509.00672

